

# Modeling and Prediction of FRP Composite Cylinder tubes Crashworthiness Characteristics

A. Khalkhali<sup>\*1</sup>, M. Afroosheh<sup>2</sup>, M. R. Seyedi<sup>3</sup>

1. Assistant Professor, 2. Ph. D. Student, 3. MSc Student, School of Automotive Engineering, Iran University of Science and Technology, Tehran, Iran

\* Corresponding Author

## Abstract

In this paper, numerical simulation of FRP composite cylinder tubes progressive crushing processes is conducted using LS-Dyna. Details on the numerical modeling strategy are given and discussed. It is found that triggers introduced in the numerical simulation can effectively model the bevel trigger at the end of the tubular specimens. It is also found that two-layer finite element model based on the TsaiWu failure criteria is effective in representing the crushing failure mode of the tubular composite specimens and energy absorption characteristics. Employing GEvoM software, two meta-models are then obtained for modeling of both the absorbed energy (E) and the peak crushing force (Fmax) with respect to geometrical design variables using input output data obtained from the finite element modeling. Comparison between obtained meta-models and numerical results in both of training and testing sets show good approximation by using obtained polynomial models.

**Keywords:** Composite cylinder tubes, Finite element analysis, Crushing behavior, GEvoM, LS-DYNA

## 1. Introduction

Due to the high specific energy absorption (SEA), carbon rein-forced composite tubes are considered as exceptionally efficient energy-absorbing components for application to aerospace and automotive structures and their SEA has been extensively investigated in recent years. To understand the damage mechanism of composite tubes, a large number of the experimental studies [1–7] have been performed. Test results indicate that the mechanism to dissipate energy is more complex than those observed in conventional materials, including matrix cracking, fiber–matrix debonding, delamination, and fiber breakage. Therefore, it is very difficult to establish an efficient and economic finite element model for predicting the energy absorption characteristics and crushing failure mode of the composite tubes.

There have been only a few published numerical studies on the axial crushing response of composite tubes. Mamalis et al. [8] developed a three-layer finite element model based on Tsai–Wu failure criteria in the LS-DYNA3D code to simulate the quasi-static axial crushing response of carbon woven fabric reinforced epoxy square tubes. This model can

effectively provide the initial peak load and the stable progressive splaying mode. But the mean crushing load and specific energy absorption predicted by this model are lower than the experimental results. Han et al. [9] established a two-layer finite element model based on Chang–Chang failure criteria in the LS-DYNA code to evaluate the crushing response and energy absorption capability of hybrid composite tubes made of unidirectional pultruded tube over wrapped with  $\pm 45^\circ$  braided fiber-reinforced plastic. In addition, McGregor et al. [10] reported that the damage propagation, failure morphology and energy absorption of braided composite tubes under axial compression, predicted by the continuum damage mechanics based on model for composite materials (CODAM), correlate well with experimental results.

In this paper, numerical simulations were performed and verified with experimental data to establish an effective model for predicting energy absorption behaviour of composite tubes. Details on the numerical modelling strategy were given and discussed. Using the FE model, parametric study was done and effects of some design parameters on the energy absorption and peak crushing force are examined. Results of such parametric study were then used as input-output data to train and test neural

network models using GEvoM software. Finally two separate polynomial models are extracted to predict energy absorption and peak crushing force of FRP composite cylinder tubes.

## 2. Numerical Simulation

### 2.1. Finite element model

To enable verification of the finite element model, quasi-static axial crushing of the composite tubes are modeled in accordance with experimental tests performed by Jung-Seok Kim [1]. The FE model which is developed using LS-DYNA is shown in Fig.1a. Loading and stationary plates of testing machine are modeled using a solid plate and a rigid plate, respectively. The composite tube was modeled using one-layer cylindrical shells as shown in Fig.1b with  $[90/0]_7$  Stacking sequence and a 0.13mm Ply thickness. The sliced tubes were nominally 100 mm in length with an inside diameter of 30 mm.

In order to decrease the computational run time, under-integrated elements (1.5 mm), four-node quadrilateral Belytschko–Tsay shell elements [2–3], were used except the elements (0.95 mm-1.5 mm) for the modelling of the bevel trigger and other three row elements (1.0 mm-1.5 mm) neighboring the bevel trigger. Fully-integrated elements were applied due to significant non-physical zero-energy deformation like hourglass shape was observed during the generation of initial crush zone. Each layer has seven through-thickness integration points representing seven different stacking lay-ups. The two horizontal translational degrees of freedom (DOFs) for the

bottom end of the tube were constrained. In addition, a planar rigid wall was defined in the location beneath the tube to ensure that the tube would always stay on the top surface of this rigid wall.

The upper end of the tube was subjected to compression by a loading platen with a constant vertical velocity 100 mm/s. In order to reduce the number of time steps, the mass density of the tube is scaled up by multiplying the original density with 1000. Furthermore, scaling up the density along with low loading velocity should ensure that the simulation represents quasi-static loading, i.e. The loading platen was modelled by a rigid plate. All DOFs of the rigid plate were constrained except for the vertical translational DOF.

The bevel trigger, chamfered on the upper end of the tubular specimen, was subdivided geometrically into one square and two isosceles right triangles, as shown in Fig. 1b. Each isosceles right triangle was modelled by one inclining element with a thickness of  $0.5t$  ( $t$  is the tube wall thickness), identical with the triangle median length. From Fig. 1b, one can see that the upper nodes of the inner layer and the outer layer were translated inward  $0.125t$ , half thickness of the inclining element, to model the  $42.3^\circ$  external chamfer that is near to  $45^\circ$ . This modelling approach of a bevel trigger is somewhat similar to the recommendations of Matzenmiller and Schweizerhof[6] as well as El-Hage[4–5] in which two or three rows of gradually reduced thickness rectangular elements with equal height were used as triggers to reduce the initial peak load and achieve a progressive crushing.

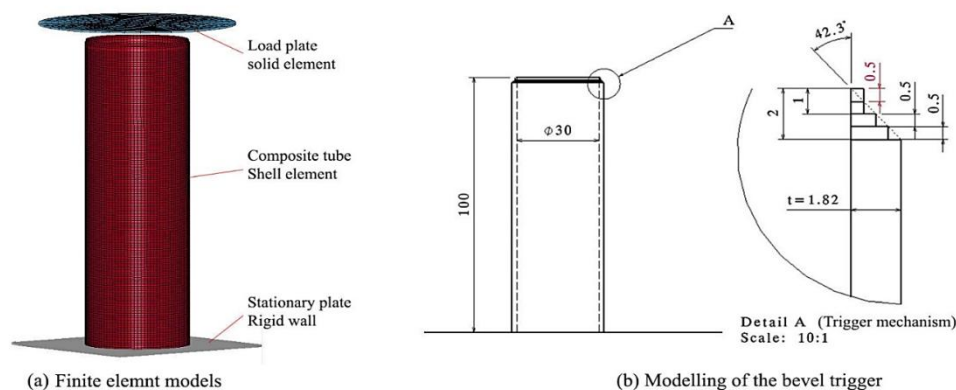


Fig1. Finite element model for axial crushing of composite tube

**Table 1.** Material properties of composites cylinder tubes

Material properties	Carbon/epoxy
Mass density ( $\text{kg/m}^3$ )	1550
Young's modulus - longitudinal direction (GPa)	127
Young's modulus - longitudinal direction (GPa)	92.3
Young's modulus - transverse direction (GPa)	0
Tensile modulus (GPa)	130(11.4)
Tensile strength (MPa)	2725(78.0)
Compressive modulus (GPa)	92.76(19.2)
Compressive strength (MPa)	551.20(69.4)
Shear modulus (GPa)	8.25(0.22)
Shear strength (MPa)	78.47(3.11)
ILSS (MPa)	71.02(0.32)

## 2.2. Damage Criteria

In the hybrid fabric composite, the carbon fibers were placed in the fill direction and Kevlar fibers in the warp direction, and thus the fill direction properties were higher than the warp direction properties with the exception of the shear properties. From the test results, the carbon/epoxy cylinder have the maximum energy absorption manner that we select it to study in this research.

The material model55 “mat\_enhanced\_composite damage” [2–3], one of the most efficient material model available for composites in LS-DYNA, was selected to represent the mechanical behavior of composite tubes. This damage criteria, valid only for thin shell elements, is based on Tsai-Wu criterion [7–8] for matrix failure. It allows users to input arbitrary orthotropic properties by specifying local material axes and appropriate constitutive constants. For completeness, the constitutive equations, the failure criteria, as well as the change of elastic material constants after ply failure encountered, are listed in what follows:

for the tensile fiber mode,

$$(\sigma_{aa} > 0) \text{ Then} \\ e_f^2 = \left(\frac{\sigma_{aa}}{x_t}\right)^2 + \beta \left(\frac{\sigma_{ab}}{s_c}\right)^2 - 1 \begin{cases} \geq 0 & \text{failed} \\ < 0 & \text{elastic} \end{cases} \\ E_a = E_b = G_{ab} = \nu_{ba} = \nu_{ab} = 0 \quad (1)$$

for the compressive fiber mode,

$$(\sigma_{aa} < 0) \text{ then } e_c^2 = \left(\frac{\sigma_{aa}}{x_c}\right)^2 - 1 \begin{cases} \geq 0 & \text{failed} \\ < 0 & \text{elastic} \end{cases}$$

$$E_a = \nu_{ba} = \nu_{ab} = 0 \quad (2)$$

The failure criterion for the tensile and compressive matrix mode is given as:

$$e_{md}^2 = \frac{\sigma_{bb}^2}{Y_t Y_c} + \left(\frac{\sigma_{ab}}{S_c}\right)^2 + \left(\frac{Y_c - Y_t}{Y_c Y_t}\right) - 1 \begin{cases} \geq 0 & \text{failed} \\ < 0 & \text{elastic} \end{cases} \quad (3)$$

For  $\beta=1$  we get the original criterion of Hashing [1980] in the tensile fiber mode. For  $\beta=0$  we get the maximum stress criterion which is found to compare better to experiments [Manual].

Table1 lists the value for material properties of the composites considered in this study, accordance with experimental tests data performed by Jung-Seok Kim [1].

## 2.3. Verification of the Numerical FE Model by Available Experimental Data

The results obtained from the FE model for the circular [90, 0] tube were compared with data of Ref [5]. Figure 2 compares the reaction force simulated by the FE model and the experimental data. In Table 2, the maximum crushing load, the mean crushing load, the total energy absorption ( $E_t$ ) and the Specific energy absorption (SEA) calculated by the model are compared with experiments. The good agreement between them confirms the validity of the model for simulating the crushing behavior of composite tubes.

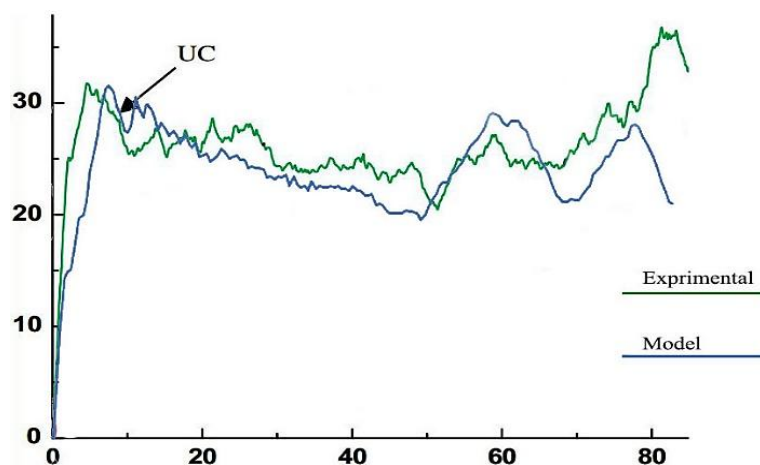


Fig2. Comparison between the reaction force given by experimental data [1] and FE model

Table 2. Comparison between numerical and experimental results [1] for a Circular Specimen with the [90/0] Lay-Up

Characteristics	Calculation	Experiment
Maximum crushing load, kN	31.4	31.3
Mean crushing load, kN	23.2	25.2
Total energy absorption ( $E_t$ ), kJ	1998	2060
Specific energy absorption (SEA), KJ/kg	71.4	72.7

### 3. Parametric Study

#### 3.1. Types of Fracture Failure

Different fiber orientation and different tube diameters had been made and their crushing behaviors were studied. Each load–displacement curve shows the history of crushing for related tube. Crushing started at a critical value which is called peak load, and then the deformation continued along the tube. Two types of fracture failure had been categorized namely, catastrophic failure and progressive failure. Catastrophic failure is presenting with high peak load followed by dropping off quickly hence the average load is low. Progressive failure absorbed more energy due to presence of multi-failure modes which lead to different characteristics of energy absorption. On the other hand, progressive failure is the opposite of catastrophic failure where by more area under the curve can be observed.

#### 3.2. Effect of Fiber Orientation on Energy Absorption

In this section, simulation results for circular tubes with 30, 45, 60 and 75mm diameter by  $\theta_1 = 0 - 90^\circ$  and  $\theta_2 = 0 - 180^\circ$  layups are presented. The fiber angles are measured from the axial direction of the tubes. We know that  $[\theta_1/0]_7$  layups is same with  $[\theta_1/180]_7$  layups, so we eliminate  $[\theta_1/180]_7$  from statistical samples. Figures 3(a, b, c, d) and 4(a, b, c, d) show the Comparison between the Maximum crushing Load and the Total energy absorption given by the FE model for different lay-ups and different diameters. As seen, the maximum force and total energy absorption increases with Diameter and reaches its maximum around the  $[90^\circ/0^\circ]$  and  $[0^\circ/90^\circ]$  layup. According to the diagrams, when  $\theta_1 = 0^\circ, 30^\circ, 60^\circ$  the maximum energies are absorbed by the tubes with  $\theta_2 = 90^\circ$  but when  $\theta_1 = 30^\circ, 60^\circ, 90^\circ$  the maximum peak loads are by the tubes with  $\theta_2 = 0^\circ$ . When  $\theta_2 = 0^\circ, 55^\circ, 125^\circ$  the maximum energies are absorbed by the tubes with  $\theta_1 = 90^\circ$  but When the  $\theta_2 = 55^\circ, 90^\circ, 125^\circ$  the maximum peak loads are by the tubes with  $\theta_1 = 0^\circ$ .

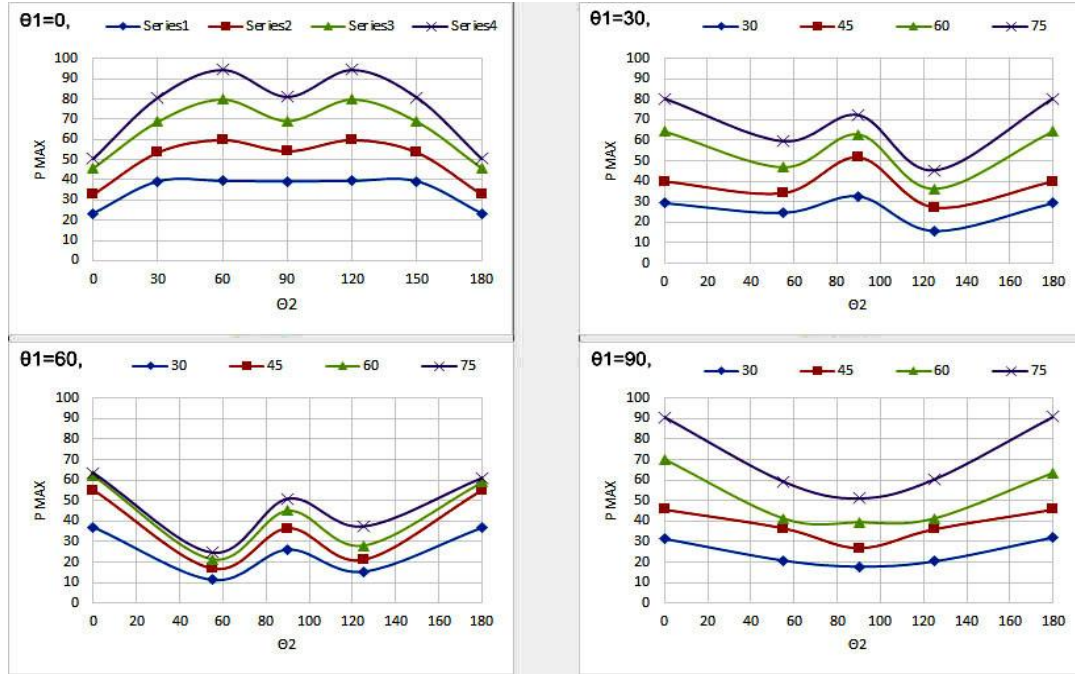


Fig 3.(a, b, c, d). Comparison between the Maximum crushing Load given by the FE model for different lay-ups and different diameter

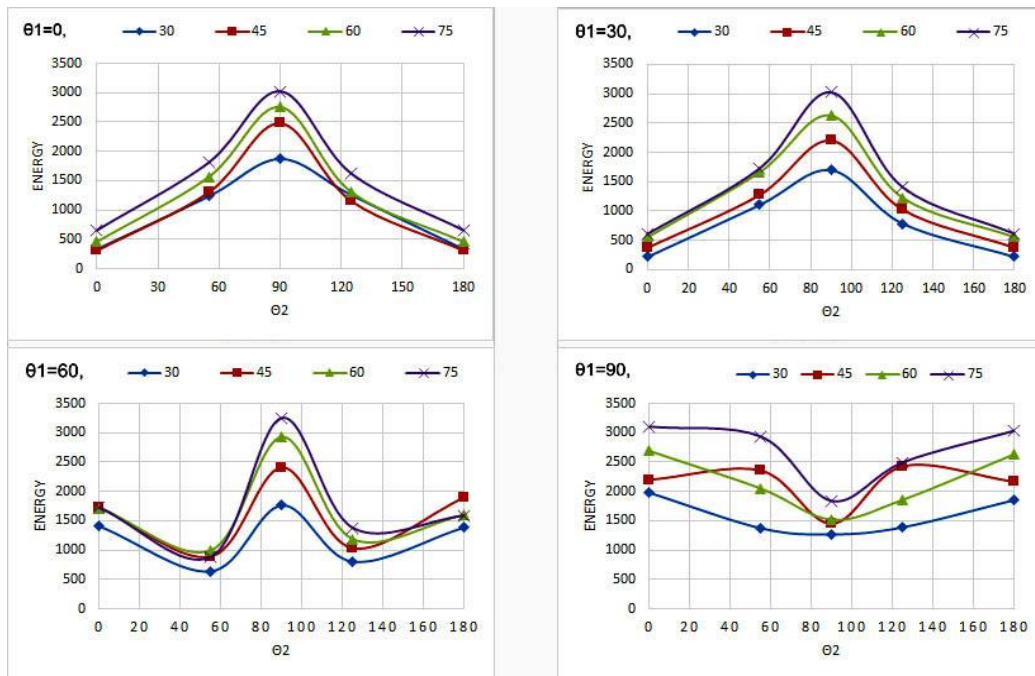


Fig 4. (a, b, c, d). Comparison between the total energy absorption given by the FE model for different lay-ups and different diameter

### 3.3. Effect of Tube Cross Section Diameter on Energy Absorption

In order to determine the amount of maximum crushing load and energy absorbed in tubes with different cross sections, circular tubes with 30, 45, 60 and 75mm diameter were considered. In Figure 5, the maximum crash load-diameter diagram for this tubes with different lay-ups are shown. It is seen that the

maximum crushing load of the circular tube with 30mm diameter happened at a lower load ( $P_{max} = 39.54 \text{ kN}$ ) than that of the 75mm diameter one ( $P_{max} = 94.42 \text{ kN}$ ).

In Figure 6, the Total energy absorption-diameter diagrams for this tube with different lay-ups are shown. It is seen that the total energy absorption of the circular tubes by majority lay-ups increases due to increasing diameter.

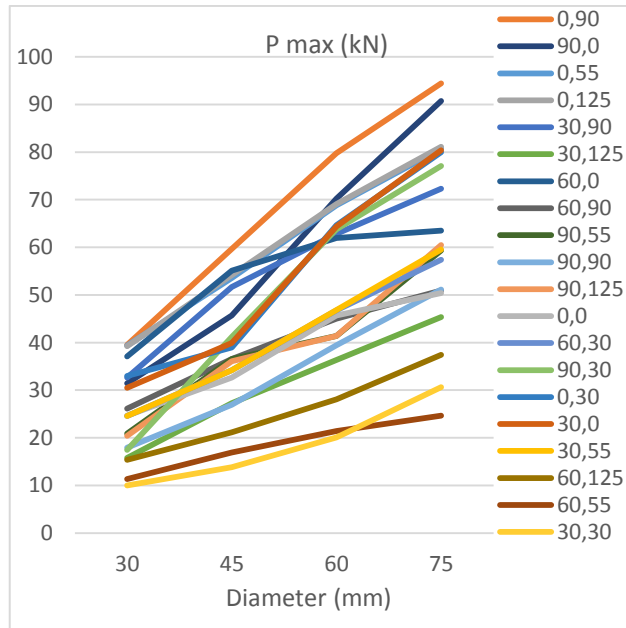


Fig 5. Comparison between the maximum crushing load given by the FE model for different lay-ups and different diameter.

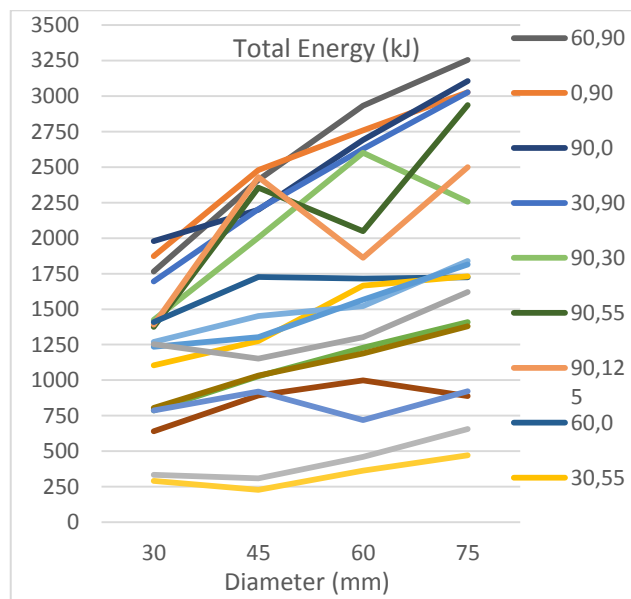


Fig. 6. Comparison between the total energy absorbed given by the FE model for different lay-ups and different diameter.

#### 4. Modeling and Prediction Using GEvoM

GMDH algorithm can be represented by the model as a set of neurons, wherein different pairs being connected by a second order polynomial, thereby generating new neurons in the next layer in each layer. This means can be used to assign the input to the output. The formal definition of the identification problem is to find a function  $\hat{f}$  that can be approximately used instead of the actual one,  $f$  in order to predict output  $\hat{y}$  for a given input vector  $X = (x_1, x_2, x_3, \dots, x_n)$  as close as possible to its actual output  $y$ . Therefore, given  $M$  observation of multi-input-single-output data pairs:

$$y_i = f(x_{i1}, x_{i2}, x_{i3}, \dots, x_{in}) \quad (i = 1, 2, \dots, M) \quad (4)$$

It is now possible to train a GMDH type neural network to predict the output values  $\hat{y}$  for any given input vector

$$X = (x_{i1}, x_{i2}, x_{i3}, \dots, x_{in}), \text{ that is:} \\ \hat{y}_i = \hat{f}(x_{i1}, x_{i2}, x_{i3}, \dots, x_{in}) \quad (i = 1, 2, \dots, M) \quad (5)$$

The problem is now to determine a GMDH type neural network so that the square of difference between the actual output and the predicted one is minimized, that is:

$$\sum_{i=1}^M [\hat{f}(x_{i1}, x_{i2}, x_{i3}, \dots, x_{in}) - y_i]^2 \rightarrow \min \quad (6)$$

General connection between inputs and output variables can be expressed by a complicated discrete form of the Volterra functional series in the form of:

$$y = a_0 + \sum_{i=1}^n a_i x_i + \sum_{i=1}^n \sum_{j=1}^n a_{ij} x_i x_j + \sum_{i=1}^n \sum_{j=1}^n \sum_{k=1}^n a_{ijk} x_i x_j x_k + \dots \quad (7)$$

Only two variables (neurons) in the form of

$$\hat{y} = G(x_i, x_j) = a_0 + a_1 x_i + a_2 x_j + a_3 x_i x_j + a_4 x_i^2 + a_5 x_j^2 \quad (8)$$

There are two main concepts involved within GMDH type neural networks design, namely, the parametric and the structural identification problems. In this way, some works by Nariman-Zadeh, et al., (2002, 2003 and 2005) present hybrid GA and singular value decomposition (SVD) method to optimally design such polynomial neural networks [11]. A non-commercial code (GEvoM) for the evolved GMDH type neural network [] has been successfully used in this paper to obtain the polynomial model of the FRP composite cylinder tubes crash behavior with minimum training errors. The obtained GMDH-type polynomial models have shown very good prediction ability of unforeseen data

pairs during the training process which will be presented in the following sections.

The input-output data pairs used in such modeling involve four different data tables obtained from numerical modeling discussed in section (2.1). The first and second tables, related to case 1 ( $D=30$ ) and case 2 ( $D=450$ ), respectively, consist of three variables as inputs, namely, two fiber angle  $\theta$  and diameter of cylinder  $D$  and one output which is the absorbed energy ( $E$ ). The third and fourth tables again related to case 1 and case 2, respectively, consists of the same four variables as inputs and another output which is the peak crushing load ( $F_{max}$ ). These tables altogether consist of the total 106 patterns which have been obtained from the finite element analysis to train such GMDH-type neural networks. However, in order to demonstrate the prediction ability of evolved GMDH-type neural networks, the data has been divided into two different sets, namely, training and testing sets. The training set, which consists of 38 out of 48 input-output data pairs for case 1 and 48 out of 58 input-output data pairs for case 2, is used for training the neural network models using the hybrid SVD and the evolutionary method of this paper. The testing set, which consists of 9 and 10 unforeseen inputs-output data samples during the training process for case 1 and case 2, respectively, is merely used for testing to show the prediction ability of such evolved GMDH-type neural network models during the training process.

The GMDH-type neural networks are now used for such input-output data to find the polynomial model of energy absorption and peak crushing load with respect to their effective input geometrical variables. In order to genetically design such GMDH-type neural network described in previous section, a population of 30 individuals with a crossover probability ( $P_c$ ) of 0.7 and mutation probability ( $P_m$ ) of 0.07 has been used in 450 generations in which no further improvement has been achieved for such population size. The corresponding polynomial representation for absorbed energy of case 1 is as follows:

$$\begin{aligned} Y_1 &= 0.491 + 24.33\theta_1 + 19.87\theta_2 - 0.021\theta_1^2 \\ &\quad + 0.032\theta_2^2 - 0.29\theta_1\theta_2 \\ Y_2 &= 5.933 - 2.31\theta_1 + 68.467D + 0.013\theta_1^2 \\ &\quad - 0.346D^2 - 0.033\theta_1 D \\ Y_3 &= 0.026 + 74.636D - 1.266Y_1 - 0.347D^2 \\ &\quad + 0.0006Y_1^2 - 0.0044Y_1 D \\ Y_4 &= -0.011 + 1.18Y_2 - 4.59\theta_2 - 4.69Y_2^2 \\ &\quad + 0.0231\theta_2^2 + 6.307Y_2\theta_2 \\ E &= 0.0043 - 0.422Y_3 + 1.504Y_4 - 0.0105Y_3^2 - \\ &\quad 0.011Y_4^2 + 0.022Y_3Y_4 \end{aligned} \quad (9)$$

Such model for absorbed energy of case 2 is represented by

$$\begin{aligned}
 Y_1 &= -1059.03 + 311.979n - 11.705D \\
 &\quad - 17.083n^2 - 0.153D^2 \\
 &\quad + 8.354nD \\
 Y_2 &= 0.019 + 1.067Y_1 + 7.011\theta_1 - 8.78Y_1^2 \\
 &\quad - 0.12\theta_1^2 - 0.0004\theta_1Y_1 \\
 Y_3 &= 0.0986 + 0.928Y_1 + 4.066D + 1.578Y_1^2 \\
 &\quad - 0.0356D^2 - 0.00027Y_1D \\
 E &= 0.0028 - 2.176Y_2 + 3.535Y_3 - 0.014Y_2^2 - \\
 &\quad 0.0142Y_3^2 + 0.028Y_2Y_3 \quad (10)
 \end{aligned}$$

Similarly, the corresponding polynomial representations to model the peak crushing load of case 1 are in the form of

$$\begin{aligned}
 Y_1 &= 0.0079 + 0.324\theta_1 + 0.39\theta_2 + 0.002\theta_1^2 \\
 &\quad + 0.002\theta_2^2 - 0.0086\theta_1\theta_2 \\
 Y_2 &= 11.075 - 0.183\theta_2 + 0.777D + 0.001\theta_2^2 \\
 &\quad + 0.0018D^2 - 0.00037\theta_2D \\
 Y_3 &= -33.812 - 0.153D + 1.986Y_1 + 0.0018D^2 \\
 &\quad - 0.023Y_1^2 + 0.0236Y_1D \\
 Y_4 &= 12.109 + 0.927Y_2 - 0.363\theta_1 + 0.0053Y_2^2 \\
 &\quad + 0.0032\theta_1^2 - 0.004Y_2\theta_1 \\
 P_{max} &= -2.77 + 0.447Y_3 + 0.728Y_4 - 0.11Y_3^2 - \\
 &\quad 0.122Y_4^2 + 0.232Y_3Y_4 \quad (11)
 \end{aligned}$$

and for the case 2 are

$$\begin{aligned}
 Y_1 &= 56.83 - 14.645n + 0.0722D + 0.875n^2 \\
 &\quad - 0.0033D^2 + 0.154nD
 \end{aligned}$$

$$\begin{aligned}
 Y_2 &= 48.166 - 4.583n - 0.188\theta_1 + 0.875n^2 \\
 &\quad + 0.0041\theta_1^2 - 0.0694n\theta_1
 \end{aligned}$$

$$\begin{aligned}
 Y_3 &= 1.471 + 1.405Y_1 - 0.3345\theta_1 - 0.0002Y_1^2 \\
 &\quad + 0.0041\theta_1^2 - 0.0085Y_1\theta_1
 \end{aligned}$$

$$\begin{aligned}
 Y_4 &= 26.759 + 0.2736D - 1.272Y_2 - 0.0033D^2 \\
 &\quad + 0.0122Y_2^2 + 0.0216DY_2
 \end{aligned}$$

$$\begin{aligned}
 P_{max} &= -3.614 + 3.263Y_3 - 2.024Y_4 - 0.182Y_3^2 - \\
 &\quad 0.124Y_4^2 + 0.304Y_3Y_4 \quad (12)
 \end{aligned}$$

The very good behavior of such GMDH-type neural network models for energy absorption are also depicted in figures 7 and 8 both for training and testing data of case 1 and case 2, respectively. Such behaviors have also been shown for peak crushing force both for training and testing data of case 1 and case 2, in figures 9 and 10, respectively. It is evident from these figures that the evolved GMDH-type neural network in terms of simple polynomial equations can successfully model and predict the output of testing data that have not been used during the training process.

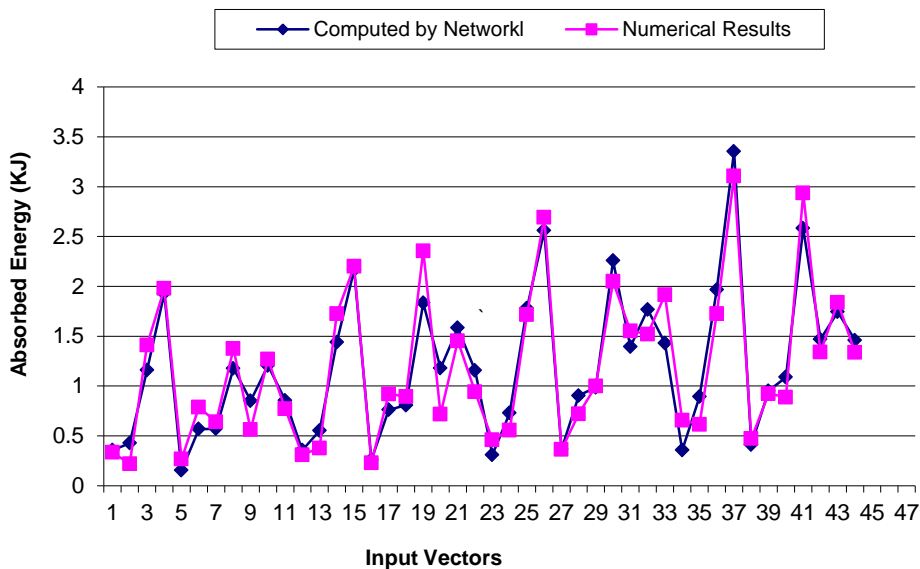


Fig 7. Variations of the absorbed energy with input data for case 1.



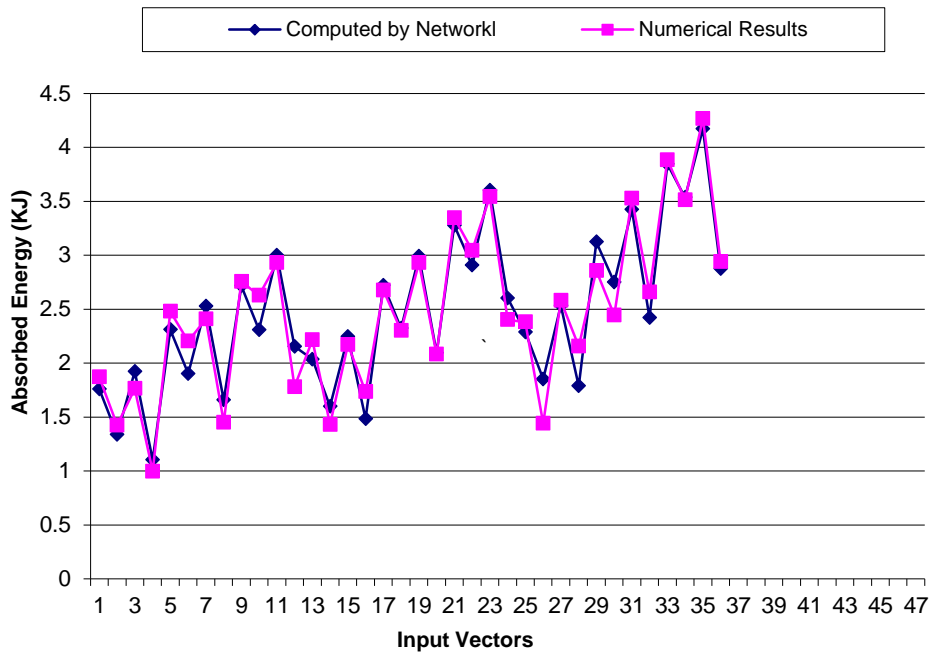


Fig.8. Variations of the absorbed energy with input data for case 2.

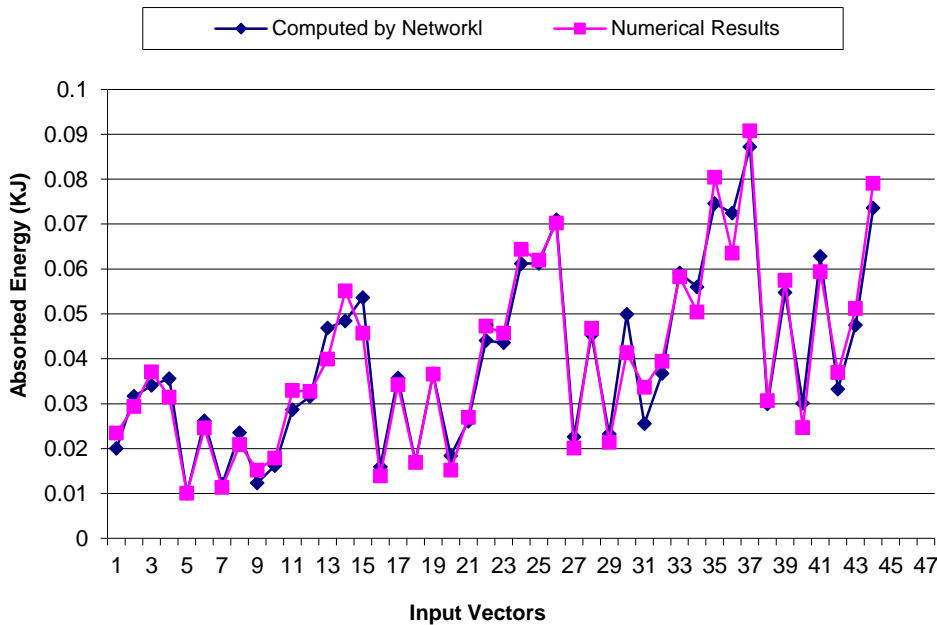


Fig.9. Variations of the peak crushing force with input data for case 1.

Downloaded from www.iust.ac.ir at 19:31 IRST on Friday March 3rd 2017 [Downloaded from www.iust.ac.ir on 2025-02-20]

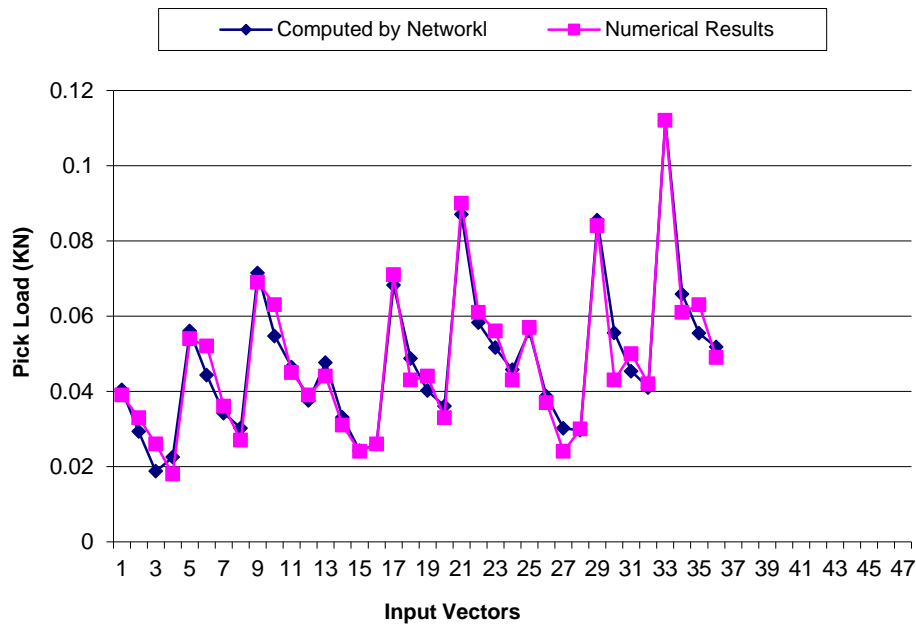


Fig. 10. Variations of the peak crushing force with input data for case 2.

The models obtained in this section are now utilized for a Pareto multi-objective crashworthiness optimization of composite cylinder tubes considering the energy absorption (E), weight of structure (W), and peak crushing load (Fmax) as conflicting objectives. Such study may unveil some interesting and important optimal design principles that would not have been obtained without the use of a multi-objective optimization approach.

## 5. Conclusion

In the present research, a finite-element modeling of the axial crushing behavior and the energy absorption of composite tubes with a different  $[\theta_1/\theta_2]$  lay-up configuration by using the LS-DYNA code is presented. The predicted damage propagation, force-displacement profile, and specific energy absorption trends agreed very well with the experiments. Based on the obtained parametric study results, the conclusions can be summarized as follows.

In the case of composite tubes with  $[\theta_1/\theta_2]$  lay-up, the maximum force arises in those  $\theta_1 = 90$  and  $\theta_2 = 0$  or  $\theta_1 = 0$  and  $\theta_2 = 90$ .

For composite tubes with the  $\theta_1$  and  $\theta_2 < 45^\circ$ , damage occurs under catastrophic failure mode.

The minimum load and energy is absorbed by those with the  $[\theta/\pm\theta]$  lay-up.

Finally some polynomials with good modeling and prediction behavior are obtained using GEvoM.

## References

- [1]. J. S. Kima, H. J. Yoon, K. B. Shin, "A Study on Crushing Behaviors of Composite Circular Tubes with Different Reinforcing Fibers". *International Journal of Impact Engineering* 38 (2011) 198-207
- [2]. Shokrieh, M. M.; Tozandehjani, H.; Omid, M. J., "Effect of fiber orientation and cross section of composite tubes on their energy absorption ability in axial dynamic loading". *Mechanics of Composite Materials*; Nov 2009, Vol. 45 (2011) 198-207
- [3]. Carla McGregor a, Reza Vaziri a, Xinran Xiao, "Finite element modelling of the progressive crushing of braided composite tubes under axial impact". *International Journal of Impact Engineering* 37 (2010) 662-672
- [4]. J. Huang, X. Wang, Numerical and experimental investigations on the axial crushing response of composite tubes. *Composite Structures* 91 (2009) 222-228
- [5]. Chiara Bisagni, "Experimental investigation of the collapse modes and energy absorption characteristics of composite tubes". Dipartimento di Ingegneria Aerospaziale, Politecnico di Milano, 28 Jul 2009
- [6]. Saijod T.W. Lau, M.R. Said, Mohd Yuhazri Yaakob, "On the effect of geometrical designs

- and failure modes in composite axial crushing”: A literature review, *Composite Structures*, Volume 94, Issue 3, February 2012, 803-812
- [7]. Finite Element Study of Energy Absorbion Characteristics of a Hubrid Structure - Composite Wrapped on a Square Metal Tube.
- [8]. S. Palanivelu, W. V. Paepegem, J. Degrieck, J. Vantomme, D. Kakogiannis, J. V. Ackeren, D. V. Hemelrijck, J. Wastiels, “Crushing and energy absorbion performance of different geometrical shapes of small-scale glass/polyester composite tubes under quasi-static loading conditions”, *Composite Structures*, Volume 93, January 2011, 992-1007
- [9]. LS-DYNA Keyword User's Manual VolumeI May 2007 Version 971
- [10]. F. Kalantary, H. Ardalan, N. Nariman-Zadeh, “An investigation on the Su–NSPT correlation using GMDH type neural networks and genetic algorithms”, *Engineering Geology*, Volume 104, Issues 1–2, 24 February 2009, 144-155
- [11]. Nariman-Zadeh, N., Darvizeh, A., Ahmad-Zadeh, G.R. (2003) Hybrid Genetic Design of GMDH-Type Neural Networks Using Singular Value Decomposition for Modelling and Prediction of the Explosive Cutting Process. *Proceedings of the I MECH E Part B Journal of Engineering Manufacture*, Volume: 217, Page: 779 – 790
- [12]. <http://research.guilan.ac.ir/gevom>